

Exciton states and tunneling in annealed semimagnetic Cd(Mn,Mg)Te asymmetric double quantum wells

S. V. Zaitsev,* A. S. Brichkin, and P. S. Dorozhkin
Institute of Solid State Physics, RAS, 142432, Chernogolovka, Russia

Yu. A. Tarakanov

A. F. Ioffe Physico-Technical Institute, Russian Academy of Science, 194021 St. Petersburg, Russia

Exciton level structure and interwell relaxation are studied in Cd(Mn,Mg)Te-based asymmetric double quantum wells (ADQWs) in normal to plane magnetic fields up to $B = 10$ T by a steady-state optical spectroscopy. As grown structures with nonmagnetic CdTe quantum wells (QWs) were subjected to quick temperature annealing to introduce Mn and Mg atoms from the barriers inside the wells resulting in formation of magnetic (MW) and nonmagnetic (NMW) QWs, respectively, with the concentration of diffused atoms of about 3–5%. A significant change of exciton energies occurs with magnetic field: at low fields exciton, localized in the MW, is higher in energy than that localized in the NMW and efficient exciton relaxation from the MW to the NMW takes place for all ADQWs. In all structures the giant Zeeman effect in the MW changes the energy order of σ^+ -polarized heavy hole (hh) excitons, localized in different wells, at high B . Levels' crossing is accompanied by a reverse of tunneling direction without anticrossing. Calculations of single-particle states and their change with B indicate that the interwell exciton transfer is forbidden in the single-particle picture at $B \gtrsim 1$ T for all studied structures. Experimentally, nevertheless, a very efficient interwell relaxation of excitons is found in the whole magnetic field range regardless of tunneling direction which evidences about importance of electron-hole Coulomb correlations in tunneling process. Surprisingly, stress effects are revealed only in the structure with the narrowest barrier while in ADQWs with thicker barriers stress relaxes completely. Different charge-transfer mechanism are analysed in details and elastic scattering due to strong disorder is suggested as the main tunneling mechanism of excitons with underlying influence of the valence band-mixing effects on the hh-exciton transfer in ADQWs with relaxed stress.

PACS numbers: 78.67.-n, 73.40.Gk, 75.75.+a

I. INTRODUCTION

During last two decades symmetric and asymmetric double quantum well (ADQW) nanostructures have attracted high attention due to a great variety of observed fundamental physical properties as well as high potential for application in solid state electronics^{1,2,3,4}. Among the most interesting and important phenomena are vertical carrier transfer - resonant or nonresonant tunneling and energy relaxation^{5,6}, energy level hybridization and state entanglement^{7,8}. Carrier tunneling was intensively studied in coupled quantum wells (QWs)^{9,10,11,12,13,14,15,16} and in pairs of correlated quantum dots^{17,18,19,20}. A possibility to control of the energy level positions and spatial localization of carrier states has made ADQW an excellent system for studying of the tunneling. It was found that excitonic effects are essential in tunneling process²¹. Several different mechanisms were considered to explain a big diversity of effects observed in tunneling experiments.

The exciton transfer in coupled QWs depends on (i) a single-particle, electron and hole, level mismatches (ΔE_e and ΔE_h) and (ii) an exciton transition energies mismatch ΔE_{ex} . When both ΔE_e and ΔE_h exceed longitudinal optical (LO) phonon energy $\hbar\omega_{LO}$ (21 meV in CdTe) tunneling of separate single electron and hole via two LO phonons emission is found to be very efficient^{22,23}. When such single-particle tunneling is ener-

getically forbidden for at least of one carrier, but $\Delta E_{ex} \geq 2\hbar\omega_{LO}$, nevertheless efficient tunneling of the exciton as a whole entity was observed in II-VI heterostructures^{5,24}. That was successfully explained as a two-step process involving indirect exciton as an intermediate state: strong Coulomb interaction renormalizes energy spectrum so that transitions forbidden in a single-particle picture become allowed⁵. Another interesting and theoretically important case takes place when neither electron nor hole can emit LO phonon, but $\Delta E_{ex} \geq \hbar\omega_{LO}$. In a single-particle picture, relaxation of every particle via acoustic phonon (deformation potential) is expected. This is much slower process with typical times of hundreds picoseconds^{22,25}. Alternative mechanism was theoretically considered by Michl *et al.*²³, namely a transfer of exciton as a whole entity through barrier by the emission of a single LO phonon. The process results from admixture of spatially indirect states to the exciton wave function in ADQW structures via Coulomb interaction and a strong Fröhlich coupling of carriers to the LO phonons. Exciton tunneling in such situation can dominate over the separate transfer of electrons and holes if the tunnel coupling between the wells is strong enough²³. To the best of our knowledge, this situation was realized only in a few works^{26,27}. Lawrence *et al.*²⁶ have reported that an efficient tunneling takes place also at the energy resonance of 1s exciton state of the narrow QW with a 2s

exciton state of the wide QW.

Previously resonances in exciton tunneling were found only in case of single-particle level resonances for adjacent QWs when using an external electric field to change mutual levels mismatch : for electrons^{12,13} and for holes^{14,15,16}. One should emphasize that careful comparison of the measured and calculated resonant fields have shown that resonant charge transfer actually involves excitons tunneling : changes in transfer dynamics are found at electric field values when direct and indirect transition energies become equal^{12,15,28}. These experimental observations suggest that the resonant tunneling of exciton-bound carriers is the transfer from spatially direct to indirect exciton state as was considered in details by Ferreira *et al.*^{6,29}.

Above considerations show a variety of coupling possibilities realized in ADQW. Besides very strong coupling caused by Fröhlich mechanism in sited papers^{9,24,26} it was found that exciton tunneling efficiency does not drop abruptly but remains still rather strong below one- or two-LO phonon energy threshold, gradually decreasing and saturating at small values of ΔE_{ex} . This experimental findings evidence that other transfer mechanisms are still efficient below LO phonon threshold. Some other scattering processes must induce the observed nonresonant carrier tunneling. For semiconductor heterostructures such mechanisms are quasielastic scattering through a deformation potential (acoustic phonons), ionized impurity, interface defect and interface roughness, or alloy scattering. Tunneling via acoustic phonon scattering is estimated to be orders of magnitude weaker than the polar coupling with characteristic tunneling times of about several hundreds picoseconds or even nanoseconds^{14,22,25} and usually should be ruled out. Calculations have shown that the elastic scattering mechanisms such as ionized impurity or interface defect assisted interwell transfer are rather effective and give rise to exciton tunneling times of the order of several tens picoseconds and, under certain conditions, even smaller^{12,22}.

Besides, strong influence of valence band-mixing effects on heavy hole (hh) tunneling have been predicted theoretically^{30,31} and observed experimentally^{32,33}. The importance of heavy-light hole mixing is emphasized in Ref.¹² where the authors argue that the evaluation of transfer time from spatially direct to indirect exciton states, which involves hole tunneling, cannot be done without consideration of valence band-mixing effects. Heavy-light hole mixing influence on exciton tunneling is found to be effective even at resonant excitation of the hh-exciton¹⁵. Plateau-like dependencies of tunneling time, observed between sequential resonances as a function of applied external electric field^{14,15} indicates band-mixing effects also²⁵.

One should mention another the most discussed transfer mechanism - dipole-dipole exciton interaction^{9,34,36} following the pioneering Takagahara's work³⁴. Comprehensive experimental studies³⁵, theoretical analysis and numeric calculations of different exciton transfer mech-

anisms in ADQWs including dipole-dipole interaction³⁶ have given too small transfer rates ($< 10^{-9}$ sec⁻¹), unable to explain experimentally observed values³⁵. On the other side, in elegant work by Kim *et al.*^{37,38}, high tunneling transparency was demonstrated experimentally for thick ternary AlGaAs barriers while opposite situation takes place for equivalent GaAs/AlAs digital barrier. These investigations clearly pointed to often forgotten fact that usually barrier material is an alloy semiconductor. If the alloy is inclined to clustering like GaAs in AlGaAs barriers one can expect percolation in charge transfer through low potential channels in the barrier. Simple model considered by Kim *et al.*^{37,38} confirms the conclusion.

This short review shows the dominant role of excitons in tunneling process in ADQWs but the transfer mechanism strongly depends on particular parameters and/or structure design. Nevertheless, in some experimental conditions the exact nature of the process is unclear and still under discussion.

In this paper we report the results of experimental studies of exciton level structure and its influence on charge transfer in semimagnetic CdTe/Cd(Mg,Mn)Te-based ADQWs as a function of magnetic fields and barrier width by using steady-state photoluminescence (PL) and PL excitation (PLE) spectroscopy. Great advantage of semimagnetic or, in another words, diluted magnetic semiconductors (DMS) is that a giant Zeeman effect makes possible continuous tuning of a band-gap E_g and exciton energies by external magnetic field due to strong s,p-d exchange interaction between free band carriers and localized d-states of magnetic ions³⁹. External magnetic field allows to vary the interwell coupling in the DMS ADQW after preparation, when the barrier width is fixed. We have found very efficient hh-exciton interwell relaxation in investigated ADQWs. Possible exciton-transfer mechanisms are analysed in details.

II. EXPERIMENTAL DETAILS

Cd_{0.8}Mg_{0.2}Te/CdTe/Cd_{0.8}Mg_{0.2}Te/CdTe/Cd_{0.8}Mn_{0.2}Te undoped ADQWs were grown by molecular beam epitaxy on thick CdTe buffer deposited on (001)-oriented CdZnTe substrate (Fig. 1). As-grown structures have two nonmagnetic pure 6-nm wide CdTe QWs separated by Cd_{0.8}Mg_{0.2}Te barrier with L_B= 3, 4 and 6 nm.

Effective thermal inter-diffusion between the barriers and CdTe QWs is promoted by use of SiO₂ upper mask and subsequent rapid temperature annealing (RTA) once (L_B= 3 and 6 nm) or two times (L_B= 4 nm) at 400 °C for one minute to promote diffusion of Mn and Mg atoms from the barriers into the QWs. 80 nm thick SiO₂ mask was deposited by electron beam lithography and lift-off after procedure. As we reported previously, diffusion is strongly enhanced below the SiO₂ mask as compared to non-covered areas⁴² and results in the increase of band-gap below the masked areas, inducing a lateral confine-

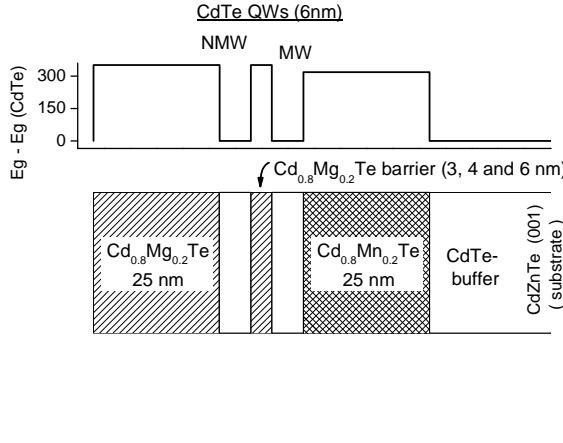


FIG. 1: Outline and band gap alignment of as grown ADQW structures.

ment potential up to 0.3 eV⁴² depending on the sample and processing parameters. It was shown that RTA technique allows to vary the QW energy gap in a controllable way with a good optical quality^{40,41,42}. QW, located between two CdMgTe barriers, incorporates only Mg atoms after RTA and is referred to as nonmagnetic well (NMW) whereas that with CdMnTe barrier contains both Mg and Mn atoms and is referred to as magnetic well (MW).

Measurements were done in superfluid He (bath temperature $T \simeq 1.8$ K) in a cryostat with superconducting magnet in Faraday geometry. Dye-laser (Pyridin1 dye), pumped by continuous Ar⁺-ion laser, was used for excitation. Circularly polarized (σ^\pm) laser beam and photoluminescence (PL) signal were formed with quarter-wave plates and linear polarizers. Sample surface was covered with opaque metallic (Au) mask leaving open small holes of 50 μm size. PL spectra were detected with a double-stage 0.82 m monochromator and CCD camera. PLE spectra were recorded as a spectrally integrated signal at low-energy spectral tail of PL band versus excitation energy. Such an experimental setup was applied to minimize a stray light when recording very broad spectral bands usual for nanostructures based on ternary semiconductor materials⁴³.

Maximum dye-laser excitation power density was $\simeq 10$ W/cm² to keep reasonable signal to noise ratio and to avoid overheating which destroys sp-d interaction in DMS semiconductors³⁹. Temperature of magnetic Mn-ions spin system in the excitation spot, estimated from magnetic field dependencies of exciton energies, was about 5 K.

III. EXPERIMENTAL RESULTS

Figure 2 displays polarized magneto-PL spectra of ADQWs. Emission was excited with σ^- polarized laser

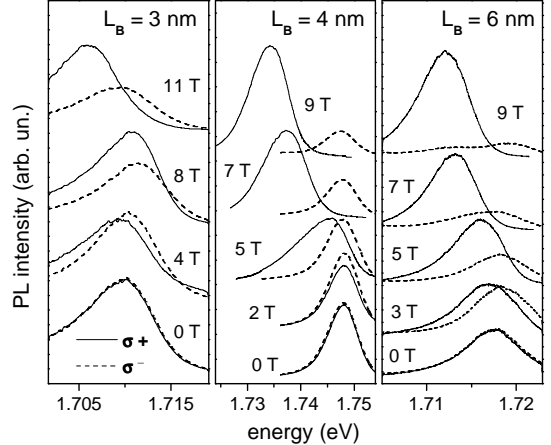


FIG. 2: Magneto-PL spectra of ADQWs with $L_B = 3, 4$ and 6 nm in Faraday geometry and intra-well σ^- -polarized excitation at ~ 100 meV above exciton transitions.

at ~ 100 meV above exciton transitions but below the barrier band gap. The spectra of all structures display broad bands with a halfwidth of 6–8 meV, characteristic for ternary II-VI materials. At low B spectral positions and line intensities are nearly B-independent in all samples, as it usually does in the NMW. At higher B, at some particular field $B_C \approx 6, 3$ and 2.5 T in samples with $L_B = 3, 4$ and 6 nm correspondingly, a red shift of the σ^+ component increases strongly while its intensity increases gradually, which is characteristic to excitons in the DMS QWs. The higher energy σ^- component, in contrast, displays a very weak shift characteristic to the NMW exciton in the whole magnetic field range. Its intensity decreases with B in all samples, the stronger decrease for ADQW with bigger L_B .

Excited exciton states were studied by the PLE. Fig. 3 represents polarized PLE spectra recorded at different magnetic fields in both polarizations. The lowest hh-exciton transition is B-independent at low fields in all structures. Thereby we ascribe it to the spatially direct transition in the NMW and label as hh (NMW) (Fig. 3). The first excited hh-exciton, labelled as hh (MW), behaves similar to that in DMS heterostructures⁴³: in σ^+ excitation polarization its energy decreases quickly with magnetic field while in σ^- polarization – increases with a giant Zeeman splitting up to 60 meV. Thereby it is ascribed to the direct transition in the MW. At some magnetic field, close to B_C , hh-exciton in the MW crosses that in the NMW. The higher exciton transitions are associated with a light hole (lh) in the MW and NMW QWs. No evidence of Landau level formation is found till $B = 12$ T as expected for QWs with strong potential fluctuations.

Magnetic field dependencies of the exciton transition energies in both circular polarization are summarized in

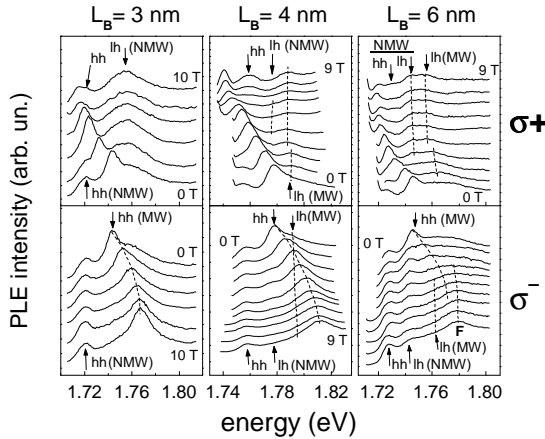


FIG. 3: Polarized PLE spectra recorded at σ^+ -polarized excitation (upper panels) and σ^- -polarized excitation (lower panels). Magnetic field increases from the bottom to the top for σ^+ polarization and vice versa for σ^- polarization with a step in 2 T for the ADQW with $L_B = 3$ nm and 1 T for ADQWs with $L_B = 4$ and 6 nm. Dashed lines are to guide the eye.

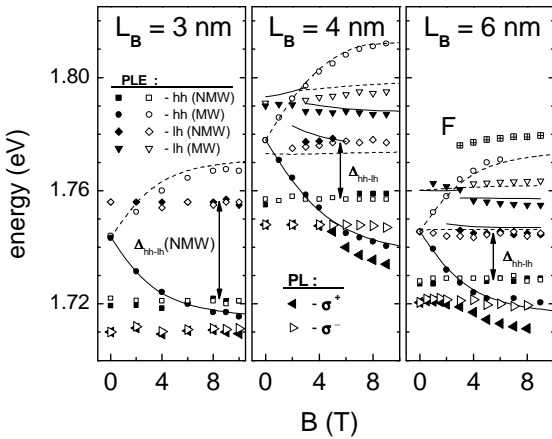


FIG. 4: Magnetic field dependencies of the exciton transition energies obtained from PLE (small symbols) and PL spectra (large symbols). Filled symbols and solid curves - for σ^+ polarization; open symbols and broken curves - for σ^- polarization; curves - are calculated dependencies acc. to the model (see text). Δ_{hh-lh} depicts hh-lh splitting in the NMW.

Fig. 4. Energies for hh and lh-exciton transitions are estimated with the accuracy of about 1 meV and 2 meV, respectively, because of the broad inhomogeneous spectral width of exciton bands. Nevertheless, systematic change of exciton energies with magnetic field can be determined and comparison with calculated dependencies can be made.

Spatially indirect hh-excitons have not been observed

both in PL and PLE spectra even in the structure with smallest L_B . On the other hand, it is known that the energy of indirect exciton in DMS ADQW is very sensitive to the structure parameters⁴⁴. On the whole PL and PLE data for the ground exciton transitions agree with each other with the values of stokes shift of 7–9 meV.

IV. DISCUSSION

A. General remarks

Spectral band, assigned to the hh-exciton of MW, splits in magnetic field into two components with opposite, σ^+ and σ^- , polarizations corresponding to $J = +1$ and $J = -1$ states of bright excitons⁴⁵. $J = +1$ and $J = -1$ excitons in PLE spectra demonstrate the giant Zeeman effect in the MW well up to 60 meV with a saturation at high magnetic fields (Fig. 4). Thus, a diffusion process during RTA treatment gives rise to a significant concentration of magnetic Mn atoms in the MW. The main contribution in splitting is provided by the strong sp-d exchange interaction of electrons and holes in semi-magnetic CdMnTe QWs with localized Mn^{2+} magnetic moments⁴³. As a result, the giant Zeeman splitting of σ^+ and σ^- polarized excitons in DMS semiconductors up to hundreds meV takes place with a huge negative g_{hh} and positive g_e effective g-factors of the heavy hole and electron, respectively³⁹.

Ground exciton transition in the MW at $B > 0$ is σ^+ polarized⁴³ and corresponds to optical transition between the upmost state with $J_z = -3/2$ moment projection in the valence band Γ_8 (heavy hole state) and the lowest state with $S_z = -1/2$ spin projection in the conductivity band Γ_6 . Very quick, till a picosecond time scale, carriers relaxation from the excited states, spin-split at finite B , to the ground one is induced by the strong sp-d exchange interactions between free carriers and Mn^{2+} ions^{46,47} and usually gives rise to observation in PL of only σ^+ polarized exciton transition at $B \gtrsim 1$ T both in 3D and 2D situation.

As a test of the used PLE methodic we recorded PLE spectra at different spectrometer positions and have not found noticeable difference in spectra shape except of intensity. According to the Ref.⁴⁸ this finding points to the absence of long-range localizing potential while very broad exciton bands (6–8 meV) evidence for a short-range disorder due to interface and/or alloy fluctuations, naturally expected in the investigated ADQWs after RTA treatment.

Strong Zeeman shift, observed for the MW exciton transition, evidences about high effectiveness of the interdiffusion between the barriers and CdTe QWs, promoted by the RTA and enhanced by using of the SiO_2 upper mask. Good optical quality as compare to the other as-grown II-VI ternary QW heterostructures^{5,24} shows up perspectives of this technology for controllable engineering of optical properties in nanostructures. For our pur-

poses the possibility to vary the interwell coupling and mutual exciton levels in such ADQWs by the external magnetic field, when the structure parameters are fixed after preparation, allows to study interwell exciton tunneling.

B. Interwell exciton relaxation

At low magnetic fields ($B < B_C$) most of the exciton recombination is observed at the lowest in energy NMW exciton transition at nonresonant excitation (Fig. 2). PLE data demonstrate that at resonant excitation of the MW hh-exciton an effective interwell exciton transfer takes place since the MW and NMW hh-exciton bands have comparable intensities in the PLE spectra (Fig. 3). This finding evidences that the interwell relaxation time of excitons, excited in the MW, is markedly smaller than their recombination time and during lifetime they mostly relax to the NMW. Above the crossing field B_C , a transfer in the opposite direction also takes place due to the same reason (PLE signal is detected at the tale of the MW PL band). Though hh-exciton, attributed to the NMW, is less pronounced at $B > B_C$ in PLE spectra with σ^+ polarized excitation because of strong spectral bands overlap and broadening, it is clearly seen in σ^- excited PLE spectra (Fig. 3). Exciton levels crossing at B_C in σ^+ polarization is accompanied by a reverse of tunneling direction without spectral peculiarities in the crossing point. Absence of anticrossing behaviour points to the absence of hh-exciton level interaction and, thus, to an incoherent nature of exciton tunneling²¹.

C. Band alignment and energy levels calculations

To understand behavior of exciton transitions and interwell exciton tunneling in magnetic field we have performed numeric calculations of single-particle energies in Γ point (zero in-plane wavevector) in the investigated ADQWs. Wave functions and level energies were obtained by solving of Schrodinger equation with appropriate boundary conditions. Band gap dependencies of E_g of $\text{Cd}_{1-x}\text{Mg}_x\text{Te}$ and $\text{Cd}_{1-x}\text{Mn}_x\text{Te}$ on the Mg and Mn concentrations are known from Ref.⁴³, while the change of E_g with magnetic field in the DMS barrier and in the MW are described by a modified Brillouin function with accurately tabulated parameters of the sp-d exchange interactions in $\text{Cd}_{1-x}\text{Mn}_x\text{Te}$ ^{39,43}. Effective electron, heavy- and light-hole masses are taken from Ref.⁴⁹. Conduction-to-valence band offset for $\text{Cd}(\text{Mn,Mg})\text{Te}$ heterostructures has been shown to obey usual for II-VI compounds 2:1 ratio rule⁴⁹. In our calculations the potential profiles of conductivity and valence bands were approximated by the rectangular shape. Though this approximation is rather simple because real concentration profiles of Mn and Mg after RTA treatment depend on the growth conditions and post-grown treatment^{50,51,52}, it allows to de-

scribe well the experimental data as will be shown below. Stress induced band shifts are used as adjustable parameters. We also neglect a small Zeeman splitting in the NMW (≈ 1 meV at $B = 10$ T)⁵³ - markedly smaller than the PLE bands spectral linewidth.

Concentrations of diffused Mn in the MW (x_{Mn}) and Mg atoms in the NMW (x_{Mg}) are evaluated from the shifts of exciton transition energies above the pure CdTe QW states in both wells at $B = 0$ T and, also, from a fit of magnetic field dependencies of hh-exciton transition in the MW. They are found to be: $x_{Mn} \approx 3.0, 5.1$ and 3.1 and $\% x_{Mg} \approx 4.1, 5.2$ and 4.4 % for samples with barrier 3, 4 and 6 nm correspondingly.

Excitonic effects such as binding energy and oscillator strength are known to be strongly enhanced in II-VI heterostructures⁴⁵ due to confinement. Modification of ADQW potential profile with magnetic field and successive change of confinement must influence on the exciton intensities and binding energies. In calculations of the exciton binding energies we have used general formulas derived in Ref.⁵⁴ and valid for an arbitrary confinement potential, which are shown to give good accuracy (less than 1 meV) also in the case of strongly coupled ADQWs. This approach is exact only at zero magnetic field, systematically underestimating exciton binding energy with increasing B , especially at high fields, when magnetic length l_B is comparable with the in-plane exciton radius⁴⁵. Nevertheless, because the exciton in-plane radius is ≈ 7 nm in all ADQWs, according to variational estimations basing on the Ref.⁵⁴, and becomes comparable with l_B only at $B \approx 13$ T, used approach allows to track qualitatively and even semi-quantitatively changing of the exciton binding energy with B in the field dependent potential.

D. Results of calculations

Calculated potential profiles of $S_z = -1/2$ conductivity and $J_z = -3/2$ valence bands, wave functions and single-particle energy levels, corresponding to σ^+ polarization of optical transition, are presented in Fig. 5 for the ADQW with $L_B = 4$ nm at three values of magnetic field: $B = 0, 2$ and 6 T (below and above B_C). At zero field both electron and hh ground states, localized in the MW, are higher in energy than those in the NMW. The giant Zeeman effect in the MW and DMS barrier dramatically decreases band energies with the main change in the valence band as the exchange interaction constant is four times stronger for hh states than that for the electron in the CdMnTe³⁹. The hh levels of the DMS and NMWs cross each other at some specific field value $B_H \approx 1$ T.

Calculated magnetic field dependencies of the single-particle ground and first excited state energies for electron (e1,e2), heavy (hh1,hh2) and light hole (lh1,lh2) in both spin states are presented in Fig. 6 for ADQWs with $L_B = 4$ and 6 nm. The energies are given relatively to

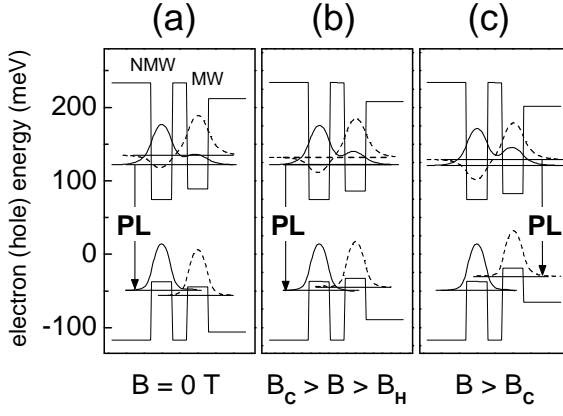


FIG. 5: Calculated electron and hole band potential profiles for $S_z = -1/2$ and $J_z = -3/2$ states, corresponding to σ^+ -polarized optical transitions, for ADQW with $L_B = 4$ nm at $B = 0$ (a), 2 (b) and 6 T (c). Electron and hole wave functions in the NM QW (solid lines) and NMW QW (dashed lines) are shifted according to state energy. Arrows indicate observed PL transitions.

the conductivity and valence band edges of bulk CdTe. These particular ADQWs are chosen for detailed analysis and comparison with the experiment because they are supposed to be unstressed as will be discussed below. For the ADQWs with $L_B = 3$ nm the dependencies of the electron and hh levels are qualitatively same as in another structures with the exception of the lh levels which are split much more (Fig. 4).

Figure 6 shows that hh levels of the MW and NMW with $J_z = -3/2$ reverse their sequence with magnetic field due to the giant Zeeman effect in the MW at $B_H \approx 1.0$ T in both ADQWs. No levels crossing is found for the electrons: the ground electron level e1, mainly localized in the NMW, has lower energy than level e2, localized in the MW, in the whole magnetic field range (Fig. 6).

Figure 7(a) presents integrated squares of corresponding wave functions $\Psi_e(z)$ and $\Psi_h(z)$ (probabilities) for electrons and hh (left panel) and lh states (right panel) in the regions of the NMW and MW for the ADQW with $L_B = 4$ nm. Hole spin representation is used below - the hole "spin" projection is opposite to the moment projection of the state in the valence band Γ_8 . Calculations show that heavy holes are effectively decoupled in adjacent wells: probability P_{leak} not to be in its "own" well is less than 10^{-4} except of a very narrow region of B near B_H . Moreover, hh states are strongly localized even in the ADQW with the narrowest barrier $L_B = 3$ nm: $P_{\text{leak}} < 10^{-3}$. Contrary, electrons and lh states with $J_z^h = +1/2$ demonstrate strong coupling. Besides, with increasing B these light holes change their location to the opposite QWs gradually, in a very wide magnetic field range 1 – 8 T (Fig. 7(a), right panel), following band

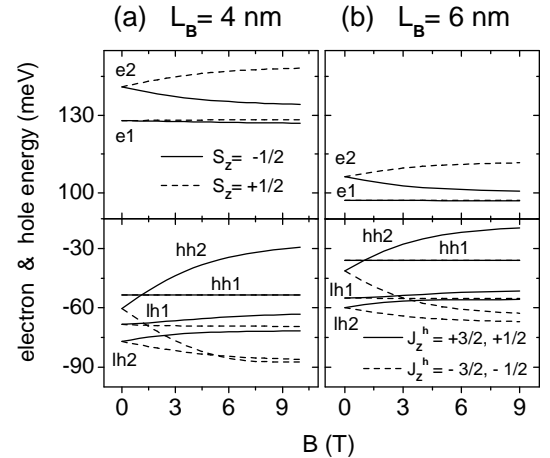


FIG. 6: Calculated magnetic field dependencies of single-particle ground and 1st excited state energies (relatively to the band edges of pure CdTe) for electrons (e1,e2), heavy (hh1, hh2) and light holes (lh1, lh2) for ADQWs with $L_B = 4$ (a) and 6 nm (b). Spin states are marked in figure. Solid lines correspond to states for σ^+ -polarized optical transitions, broken lines - for σ^- .

gap shrinkage in the MW, but still having a significant probability to be in the opposite well: $P_{\text{leak}} > 4\%$ at high fields. Light holes with opposite spin $J_z^h = -1/2$ preserve original, same to $B = 0$ T, localization. Such behavior reflects delocalized nature of light holes in investigated ADQWs due to much smaller value of a lh mass in the quantization direction⁴⁹ and smaller barrier value for the lh states.

Exciton binding energies as a function of magnetic field are shown in Fig. 7(b) for σ^+ polarized hh-excitons for all ADQWs (left panel) and for lh-excitons in the ADQW with $L_B = 4$ nm (right panel). Interestingly, it turned out that in each ADQW binding energies of hh exciton in the MW and NMW have very close values in the whole magnetic field range (the difference is less than 0.5 meV) which is caused by strong hh confinement. One can see a strong influence of the spatial localization on the binding energy: first, hh-excitons in ADQW with wider barrier have higher binding energy value due to stronger electron localization. Secondly, binding energy of the lh-excitons correlates with the localization degree of the light holes: the smaller overlap of lh wavefunction with electron - the lower corresponding binding energy and vice versa.

According to calculations for ADQW with $L_B = 4$ and 6 nm, NMW lh-exciton in σ^+ polarization is ascribed to e1-lh1 transition at low magnetic fields ($B < 2$ T) when both carriers are localized mainly in the NMW (Fig. 7(a)). With increasing field lh1 continuously delocalizes and changes its location to the MW. At higher fields ($B > 5$ T) e1-lh2 transition can be considered as

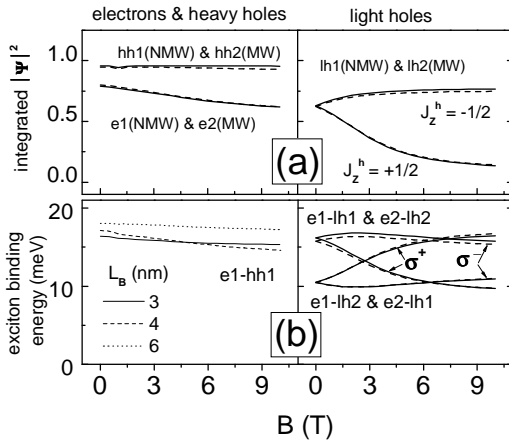


FIG. 7: (a) Integrated squares of wave functions $\Psi_e(z)$ and $\Psi_h(z)$ vs B for electrons and hh (left panel) and lh states (right panel) in the regions of the NMW and MW (marked in figure) for ADQW with $L_B = 4$ nm. (b) Exciton binding energies for σ^+ -polarized hh-excitons (left panel, all ADQWs) and lh-excitons in the ADQW with $L_B = 4$ nm (right panel). e1-lh1 and e1-lh2 (e2-lh2 and e2-lh1) excitons are shown by solid (dashed) lines, respectively. σ^+ (σ^-) exciton polarizations are marked in figure.

the NMW lh-exciton because in this field range lh2 level changes its localization to the NMW while e1 state is always mostly localized in the NMW (and e2 - in the MW). In σ^- polarization, like zero field situation, e1-lh1 transition is being the NMW lh-exciton because for these carrier spin states band profile doesn't change relative QWs alignment, preserving carrier localization.

Similarly, the identification of lh-exciton can be done in the MW. For this exciton transition lh1 and lh2 levels interaction is seen most prominently. According to calculations, MW lh-exciton at low B starts as e2-h2 transition, when both carriers are localized mainly in the MW, and have the highest transition energy. At higher fields ($B > 3$ T) MW exciton in σ^+ polarization quickly decreases its energy and can be assigned to e2-lh1 transition in accordance with the change of lh localization. In σ^- polarization the MW lh-exciton is ascribed to e2-lh2 transition at all B because both carriers are localized in the MW.

Calculated lh-exciton transition energies for discussed ADQWs with $L_B = 4$ and 6 nm are depicted together with experimental ones in Fig. 4. Data for the lh-excitons are presented in the field regions where they have significant intensities according to the above discussion. One can see rather satisfactory agreement between calculated values and measured ones with worse agreement for the lh-excitons. Is not surprising for the hh-excitons because model parameters were chosen to fit their experimentally found energies. As to the lh-excitons, comparison with the experiment is complicated due to broad spectral

width of exciton bands in PLE and smaller value of lh microscopic transition matrix elements as compare to hh transitions⁴⁵. Four possible combinations of light hole excitons in every polarization (two electrons times two lh holes) are reduced to only two strong transition at low and high magnetic fields due to definite localization of the light holes thus complicating analysis only at middle B values. Analysis can be entangled also by interplay between intrawell and interwell exciton relaxation kinetics and reversing of exciton transfer direction between QWs at B_C . As an example of such an ambiguity, in the ADQW with $L_B = 4$ nm it is difficult to identify the NMW lh-exciton transition in σ^+ polarization whereas it is clearly seen in σ^- polarization. Contrary, in the ADQW with $L_B = 6$ nm lh-exciton from the NMW is clearly seen in both polarizations.

Calculations for the ADQW with $L_B = 3$ nm have shown that e1(NMW)-hh2(MW) indirect exciton is the ground energy state at high B . Experimentally, nevertheless, indirect exciton is not observed in this structure as well as in another ones. On the other hand, it is known that the energy of indirect exciton in DMS ADQWs is very sensitive to the structure parameters⁴⁴ and we ascribe this contradiction to the weakness of calculations for the ADQW with the narrowest barrier.

In addition to identified lh-exciton transitions Fig. 3(c) displays σ^- polarized transition arising at $B > 4$ T for the ADQW with $L_B = 6$ nm (noted as F). It cannot be assigned to transitions with participation of higher electron or hole levels because they have much higher energies. We suppose that it appears due to hh-lh valence band-mixing between hh2 ($J_z^h = -3/2$) and lh2 ($J_z^h = -1/2$) levels, localized in the MW and converging at high fields (Fig. 6). Another evidence for such a mixing is anomalously broad MW-assigned hh-bahd in the ADQW with $L_B = 4$ nm (Fig. 3(b)) in which, according to calculations, hh2 and lh2 levels cross at high fields and stay very close (less than 3 meV at $B > 5$ T). Both hole states are localized in the MW, hh2 - completely and lh2 - with a probability $> 82\%$ and can be analyzed as first heavy and light hole states in a single QW. Symmetry analysis presented in Ref.⁵⁵ (table II therein) shows that there is only $2p^-$ lh-exciton state with the same symmetry Γ_{7g} as a ground 1shh-exciton, which can mix with 1shh in σ^- polarization. Symmetry requires also that $2p^-$ lh-exciton should have odd single-particle wave functions⁵⁵ (negative parity of the product $\Psi_e(z) * \Psi_h(z)$) and only violation of mirror symmetry in the MW can give rise to such considerable strength of optically forbidden exciton state. Another Γ_{7g} state, $3d^{\pm}lh$, has orbital moment projections $m = -3, \pm 2$ and $+1$ and doesn't couple to the σ^- -polarized optical field. We suppose it is a violated symmetry in ADQWs after RTA treatment^{51,52,56} due to two times bigger diffusion coefficient of Mn atoms than that of Mg in CdTe matrix⁵⁷ which is responsible for the origin of this band in the MW.

Thus, calculations in the simplest model with rectangular shape potential profile describe very well hh-exciton

magnetic field behavior in the studied ADQWs. As for the lh-excitons, correspondence is worse due to smaller m_{lh}^z mass and higher lh energies, inquiring knowledge of exact band potential shape. Basing on our calculations, we conclude that the heavy hole levels are completely decoupled, while light hole levels interact strongly with pronounced coupling.

E. Stress effects in annealed ADQWs

It is known that in heterostructures with a single QW stress is fully accommodated by the QW with the barriers being unstressed completely⁵⁸. In calculations of light hole energies for ADQWs with $L_B = 4$ and 6 nm the stress induced additional shift of lh levels is set to zero. Only in this case calculations provide satisfactorily description of exciton transitions considered above and, particularly, explain small values of hh-lh splitting Δ_{hh-lh} for these ADQWs (Fig. 4). Stress effects in the QWs are completely neglected only for these two particular structures except of one with $L_B = 3$ nm, where lh-exciton in the NMW is sufficiently higher split in energy: $\Delta E_{hh-lh} \approx 35$ meV. This value is much bigger than one expected without stress. Such a big splitting is a result of considerable stress inside QWs in the ADQW with the narrowest barrier.

Stress relaxation effects in the annealed ADQWs with $L_B = 4$ and 6 nm as a result of RTA treatment are in accordance with the results of thorough experimental investigations and numerical simulation of diffusion process in asymmetric CdMnTe/CdTe/CdMgTe quantum wells⁵⁹. In this work authors indicate that full stress relaxation during the RTA procedure is significant to explain their and reported by Tönnies *et al.*⁵⁷ results. To understand the experimentally observed difference of stress relaxation in ADQWs with different barriers one should suggest: (i) the stress can partly relax in the interwell barrier region, i.e., to be adopted by the barrier; (ii) the strongest relaxation occurs at some optimal barrier width comparable with the QW width, because relaxation effect should vanish in utmost cases for very narrow ($L_B = 3$ nm) as well as for very wide barriers. We don't have direct references concerning this phenomenon except of Ref.⁵⁹ and make this speculation as a suggestion to explain the experimental data. Besides, ADQW with $L_B = 4$ nm is treated twice at elevated temperature thus the stress relaxation effect for this structure should be stronger.

F. Exciton tunneling mechanisms in annealed CdTe-based ADQWs

1. Semiclassical single-particle approach

In the single-particle picture, tunneling of the heavy hole with zero in-plane hh kinetic energy from the MW

to the NMW is prohibited at $B > B_H$ since the final hole state is higher in energy. On the other hand, exciton transition in the MW has higher energy than that in the NMW until B_C and, as PLE experiment definitely shows, effective tunneling of the hh-excitons from the MW to the NMW at $B < B_C$ takes place. Vice versa, at $B > B_C$, effective hh-exciton tunneling from the NMW to the MW occurs as discussed at the beginning of this section. Electron level e1, localized in the NMW, has lower energy than that in the MW (e2) in the whole magnetic field range (Fig. 6) which prevents tunneling of the electron with zero in-plane kinetic energy from the NMW to the MW at $B > B_C$, again in contradiction with the experiment. Thus, in contrast with the single-particle picture, experiment indicates very efficient exciton transfer in the field range $B > B_H$, prohibited for the tunneling of uncorrelated free carriers. This contradiction emphasizes the importance of exciton correlation in charge transfer processes in semiconductor heterostructures and shows that the tunneling direction is governed only by the exciton transition energies in the adjacent QWs in accordance with the results of Refs.^{5,9,24,26}.

In discussing the nature of exciton transfer mechanism in investigated ADQWs, one has to mention that the semiclassical, single-particle estimation of the heavy hole tunneling time⁶⁰ gives values ≈ 8 ps, 65 ps and 2.7 ns for ADQWs with barriers $L_B = 3, 4$ and 6 nm respectively. On the other hand, free exciton radiative lifetime in CdTe/Cd(Mg,Mn)Te-based QWs falls in range of 80–150 ps depending on the QW parameters^{26,61,62}. Thus, only for ADQWs with $L_B = 3$ and 4 nm estimated tunneling times are reasonable to explain experimentally observed efficient exciton transfer during exciton lifetime, being completely unappropriate for the structure with the widest barrier of 6 nm.

To clarify the question about tunneling times in the studied ADQWs, exact calculations of the hh interwell tunneling rates (inverse tunneling times) have been done in a single-particle relaxation picture. We considered only the most reasonable in the studied undoped structures transfer mechanisms such as relaxation via the emission of the acoustic phonons²², LO phonons⁶³ and alloy fluctuation elastic scattering⁶⁴. For the alloy fluctuation elastic scattering we used the value of scattering potential of GaAs because of the absence of this value for Cd(Mn,Mg)Te compounds in the literature. Calculated dependencies of the scattering rates on the initial in-plane hh kinetic energy from the higher state hh2 to the ground state hh1, which are localized in different QWs, are depicted in Fig. 8 for $B = 0$ and 10 T. At $B = 0$ T hh tunneling takes place from the MW to the NMW while at $B = 10$ T - contrariwise. Figure 8 shows that the relaxation via acoustic phonons is much slower process with typical times of nanoseconds and thus can be neglected. One can see that the elastic alloy-disorder relaxation mechanism does't depend on the in-plane hh kinetic energy⁶⁴ and do provide transfer rates sufficient for effective interwell hh tunneling in ADQWs with $L_B = 3$ and 4 nm: calcu-

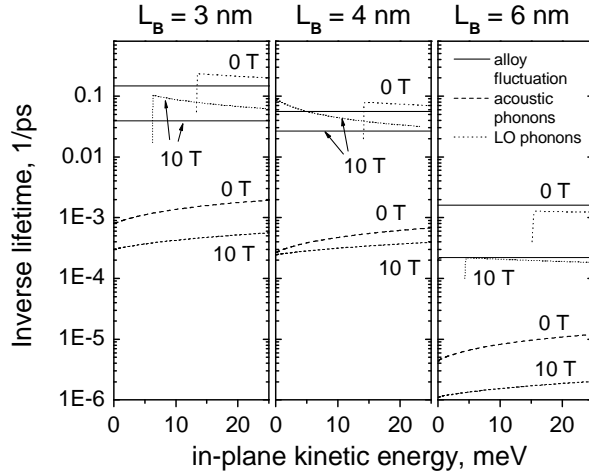


FIG. 8: Calculated dependencies of the scattering rates vs in-plane hh kinetic energy between hh₂ and hh₁ states via alloy fluctuations (solid lines), emission of the acoustic phonons (dashed lines) and LO phonons (dotted lines) at B = 0 (thick lines) and 10 T (thin lines).

lated transfer times are of about several tens picoseconds (or even smaller for the ADQW with $L_B = 3 \text{ nm}$) do not exceed typical exciton recombination times ($\sim 100 \text{ ps}$ in CdTe QWs⁶¹). Usually the strongest scattering mechanism through LO phonons in the studied structures has an energy threshold except for high B in the ADQW with $L_B = 4 \text{ nm}$ (Fig. 8(b)). According to the single-particle calculations, LO-threshold for energy difference between the hh₁ and hh₂ states in this structure vanishes at $B > 7.5 \text{ T}$ (Fig. 6(a)) which explains evident growth of the NMW hh-exciton band in the PLE spectra (Fig. 3, $L_B = 4 \text{ nm}$). As to the ADQW with $L_B = 6 \text{ nm}$, neither of the considered mechanisms can provide sufficient interwell transfer rates in agreement with simple semi-classical estimations. Thus, very weak tunnel coupling between the hh states for the widest ADQW gives rise to very low interwell transfer rates, which cannot explain efficient hh-excitons transfer, experimentally found in the presented studies.

2. Barrier quality

In our previous publications of the influence of RTA treatment on the optical properties of CdTe/(Cd,Mg)Te annealed nanostructures were investigated^{65,66}. We have not found any sign of (i) segregation phenomena in this material system and (ii) deviation of Mg diffusion from the classical linear Fick's law. Same conclusion is made in the studies of nonmagnetic CdTe/CdMgTe QWs⁶⁷. Moreover, comparative investigations of diffusion process in RTA procedure have revealed same activation energy and comparable values of Mg and Mn atoms diffusion co-

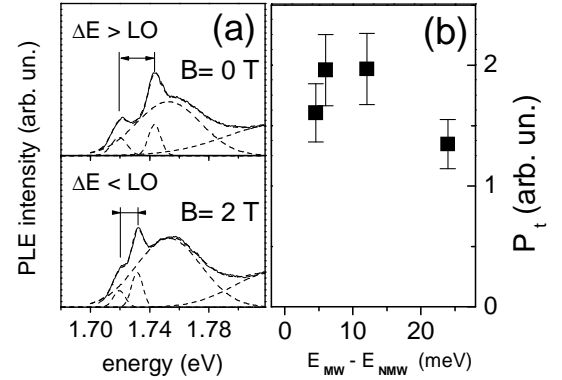


FIG. 9: (a) Spectral deconvolution by gaussians of PLE spectra for ADQW with $L_B = 3 \text{ nm}$ at B = 0 T ($\Delta E_{ex} > \hbar\omega_{LO}$) and B = 2 T ($\Delta E_{ex} < \hbar\omega_{LO}$). (b) Tunneling probability P_t from the MW to the NMW QW vs hh-excitons energy separation ΔE_{ex} .

efficient in CdTe matrix⁵⁷. In magneto-optical studies in the DMS CdTe/CdMnTe heterostructures no segregation effect of Mn was found also^{51,52,56,57,59}.

Thus, we have no hints to suppose the existence of low potential conductivity channels in the barrier, caused by alloy segregation or clustering in the investigated material system Cd(Mn,Mg)Te, similar to reported by Kim *et al.* for GaAs/AlGaAs heterostructures^{37,38}.

3. LO-phonon exciton tunneling

We have analyzed also another mechanism of the exciton tunneling as a whole entity via the emission of the LO phonon²³ which should dominate over the separate transfer of electrons and holes if the tunnel coupling of QWs is strong (small L_B). Small separation between MW and NMW hh-exciton PLE bands at high B, realized in the structure with the barrier $L_B = 3 \text{ nm}$ (Fig. 4), allows to record PLE spectra with much better quality in cross-circular polarizations. Spectral deconvolution by gaussian bands (Fig. 9(a)) makes possible to analyze tunneling efficiency between MW and NMW hh-exciton ground states depending on the exciton energy separation ΔE_{ex} . Figure 9 demonstrates that, starting at B = 0 T, where $\Delta E_{ex} > \hbar\omega_{LO}$, towards $\Delta E_{ex} = 0$ no threshold-like behavior is observed in a relative tunneling efficiency P_t , defined here as a ratio of the MW to NMW hh-exciton PLE band intensities of the hh-excitons. Oppositely, at $\Delta E_{ex} > \hbar\omega_{LO}$ value of P_t is even somewhat smaller than that at $\Delta E_{ex} < \hbar\omega_{LO}$ (Fig. 9(b)). This result excludes exciton tunneling through the emission of a single LO phonon, the mechanism theoretically considered by Michl *et al.*²³ for ADQWs with thin barriers and which has been observed experimentally only in a few experiments^{26,27}.

4. Two-step exciton tunneling mechanism

Previous investigations of tunneling phenomena in ADQWs have shown that resonant charge transfer in many cases actually involves exciton tunneling from spatially direct to indirect exciton state^{6,12,15,28,29}. On the other hand, calculations^{5,12,23} indicate that tunneling between spatially direct exciton states is normally not efficient due to very weak admixture of the direct exciton wave functions. It has been suggested that two-step tunneling scheme would work more efficiently with an indirect exciton as an intermediate state. Experiment has confirmed the effectiveness of the two-step scheme when LO phonon emission is allowed at every step thus overcoming too weak tunneling between direct exciton states⁵.

Calculations show that at low B both indirect excitons have higher energies than both direct excitons in ADQWs with $L_B = 4$ and 6 nm (Fig. 10, $L_B = 6$ nm case), i.e. the above mechanism is ineffective. The situation changes at $B > B_C^* \approx 5$ T when indirect exciton has lower energy. The lowest indirect exciton is composed of the NMW electron and MW hole, i.e. symbolically $e(\text{NMW})\text{-hh}(\text{MW})$, while another indirect exciton $e(\text{MW})\text{-hh}(\text{NMW})$ is always the highest energy exciton state (Fig. 10) and thus can be omitted as an intermediate state. First step in such exciton transfer scheme involves heavy hole tunneling $\text{hh}(\text{NMW}) \rightarrow \text{hh}(\text{MW})$. The second step involves electron tunneling $e(\text{NMW}) \rightarrow e(\text{MW})$ and it is energetically prohibited in the single-particle picture for electrons with zero in-plane kinetic energy as discussed above. But the two-particle nature of hole-assisted electron tunneling process makes it different from the ordinary one-particle (electron or hole) tunneling process⁶⁸. The prohibition can be overcome by an additional excitonic Coulombic potential which changes locally confinement potential of the heterostructure^{69,70} and may provide electron tunneling to the final, energy profitable exciton state in the MW. The analysis of the NM hh-exciton intensity in σ^- polarized PLE spectra (Fig. 3) does not show threshold behavior at $B > B_C$, which may point to the opening of the additional NMW \rightarrow MW exciton transfer channel. Thus, we do not have direct evidence of the two-step exciton tunneling at high fields.

Comparable intensities of the MW and NMW hh-excitons in PLE spectra in all studied ADQWs with big range of barrier thickness points to weak dependency of the tunneling mechanism on the L_B . Interestingly, such an independency has been found in recent time-resolved investigations in semimagnetic Zn-MnSe/ZnCdSe ADQWs⁷¹. Very long (few ns) PL decay times observed in Ref.⁷¹ rule out the possibility of free exciton tunneling and evidence for the transfer process through some kind of localized excitons or excitations. Insensitivity of the decay times to the barrier height as well as to the barrier width (4–8 nm) contradicts to the traditional exponentially dependent tunnel-

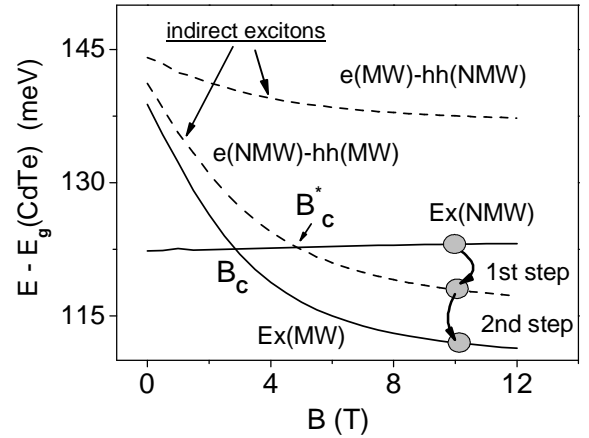


FIG. 10: Calculated magnetic field dependencies of direct ($\text{Ex}(\text{NMW})$, $\text{Ex}(\text{MW})$) and indirect ($e(\text{MW})\text{-hh}(\text{NMW})$, $e(\text{NMW})\text{-hh}(\text{MW})$) exciton energies in ADQW with $L_B = 6$ nm. Two-step exciton interwell transfer through the intermediate indirect exciton state at high B is illustrated schematically.

ing mechanism. Authors⁷¹ suggested photon-exchange energy transfer³⁶ of the localized excitons or electron-hole pairs. This mechanism is known as slowly varying with interwell distance³⁶ and that's why is regarded as the most plausible. Contrary to the PL data of Ref.⁷¹, in presented ADQWs exciton recombination from the MW is absent in PL spectra at $B < B_C$ (Fig. 2). This fact evidences about much quicker exciton transfer in the investigated ADQWs with thermally induced disorder and points to different transfer mechanism than that realized in ADQWs studied by Chen *et al.*⁷¹.

Concluding this discussion, we would like to note that, in principle, finite uncontrolled doping level in nominally undoped heterostructures supply carriers which can significantly change local potential band picture, promoting single-particle exciton tunneling with the help of carriers localized in the opposite QW. It is known^{72,73} that intrinsic defects in CdTe can provide both n- and p-doping type, with the doping level dependent on the growth conditions. High tunneling efficiency was reported⁷⁴ the in CdTe-based ADQWs with $L_B \leq 6$ nm and n-type doping concentration of the order of 10^{15} cm^{-3} . On the other hand, localized carriers would form different exciton-bound complexes which were present in the cited work⁷⁴. This is not the case in the studied structures, which do not show any pronounced PL spectral bands additional to the localized at potential fluctuations hh-exciton band (Fig. 2). Thus, we rule out major contribution to the interwell tunneling due to free/localized carriers supplied by residual impurities or/and defects.

5. Valence band-mixing effects in exciton tunneling

Stress relaxation during RTA give rise to small values of $\Delta_{hh-lh} = 19$ and 15 meV in ADQWs with $L_B = 4$ and 6 nm, respectively (Fig. 4), which are same or smaller than hh-exciton binding energies $\simeq 18$ meV (Fig. 7). As a result, valence band-mixing should be significant in definition of exciton states^{45,75}. Theoretical considerations and numeric calculations have shown that inclusion of valence band-mixing is crucial for qualitative understanding and estimation of the hole transfer rates both at on- and off-resonance conditions^{12,25,76}. Particularly, Ferreira and Bastard⁷⁶ have stressed that the rates of tunneling assisted by elastic scattering via interface defects, impurities, or alloy fluctuations, are considerably increased by the valence band-mixing effect over ones deduced without taking into account the band-mixing.

An exact solution of the single-particle hh tunneling in ADQW via acoustic phonons with accounting of the hh-lh mixing is done in Ref.²⁵. As it has been shown²⁵, relaxation rate at out-of-resonant conditions is defined by the light hole tunnel exponent and does not depend on the heavy holes levels mismatch ΔE_h when it is bigger than tunnel matrix element, in agreement with some experimental data^{14,15}. It is important that this result is valid not only for acoustic phonons scattering but also for any short-range potential scattering relevant in the case of ADQWs with essential disorder²⁵. Estimations made according to Ref.²⁵ show that in the studied ADQWs hh tunneling through the lh-mixing channel should prevail at $\Delta E_h \gtrsim 2$ meV, i.e. in the whole magnetic field range except of a narrow field interval near B_H , where resonant tunneling may prevail.

It is a decoupled model that has led to a widespread belief that hh tunnels considerably slower than electron. Without accounting of the hh-lh mixing calculated hh transfer times via elastic scatterers are of several orders longer than the observed ones¹². hh-lh coupling strongly depends upon the in-plane wave vector \mathbf{K} . Even if the initial state is a hh $\mathbf{K}=0$ state, elastic scattering via any static scatterer can couple hh to a $\mathbf{K} \neq 0$ lh state, which due to band-mixing has a nonzero projection to the other hh state⁷⁷. The importance of band-mixing effect on the interwell heavy hole tunneling was revealed in experimental studies in electrically biased ADQWs^{29,76}. Numeric calculations, made in these Refs.^{29,76}, have shown that the hole and electron transfer times assisted via the static elastic scatterers are in general comparable. Moreover, it is absolutely necessary to account for valence band-mixing for explanation of resonances in tunneling times between hh and lh states, observed in Refs.^{15,78}.

We suggest that the valence band-mixing effect is a determinant factor responsible for the observed effective exciton relaxation in the whole magnetic field range, i.e. at all discussed experimentally realized band alignment configurations. Spatial delocalization of the lh states in investigated ADQWs would promote very efficient interwell tunneling of the hh-excitons through the strong

hh-lh mixing. As for the tunneling mechanism itself we naturally suppose elastic or quasi-elastic scattering via static scatterers such as alloy composition fluctuations, in first order, interface defects and impurities, which are expected to be present in abundance in the investigated ADQWs as a result of RTA treatment and ternary composition. Exciton relaxation via acoustic phonons is of orders weaker (Fig. 8) while LO phonon assisted exciton tunneling²³ turns out to be ineffective even in the ADQW with $L_B = 3$ nm (Fig. 9). Full theoretical description of exciton tunneling via quasi-elastic scattering with taking into consideration valence band-mixing of heavy hole is not developed at present. Very interesting attempts to consider the hh-exciton tunneling problem with accounting of the exciton Coulomb correlations of the electron-hole pair have been undertaken only in several publications^{5,6,12,44} by choosing of appropriate exciton wavefunctions for initial and final carrier states but without considering of the valence band-mixing.

Strong influence of valence band-mixing effects on the exciton tunneling can be suggested from the PL experiments also (Fig. 2). σ^+ -polarized hh NMW exciton has negligible intensity at $B > B_C$ which evidences about complete transfer of excitons from this state to the MW during relaxation of photoexcited carriers. Non-resonantly excited carriers relax in two stages: after ultrafast subpicosecond energy relaxation by LO-phonon emission⁷⁹ excitons with a large center-of-mass momentum \mathbf{K} are created during first tens picoseconds⁸⁰. Then, for hundreds of picoseconds, exciton loses its excess energy through acoustic phonon emission⁸⁰. The hole acquires a part of the total exciton momentum and thus turns up in a strongly valence band mixed state. Short tunneling times of the hh-exciton as compare to the energy relaxation times (hundreds of picoseconds) are required to explain the experimental finding.

V. CONCLUSIONS

Magneto-optical properties of semimagnetic Cd(Mg,Mn)Te-based ADQWs, subjected to the quick thermal annealing, are studied. Very efficient interwell relaxation of the heavy hole excitons is observed in the whole magnetic field range regardless of the tunneling direction. Single-particle description fails to explain tunneling picture that emphasizes importance of the excitonic correlations in the tunneling processes in semiconductor heterostructures.

Main conclusions of the work are the following:

- 1) rapid temperature annealing of the ADQW with SiO₂ cap layer effectively introduce magnetic (Mn) and nonmagnetic (Mg) impurity atoms from the barriers into initially nonmagnetic CdTe QWs with a good optical quality. It allows to control mutual carrier levels alignment and energy order of the intrawell exciton transitions in such ADQWs by the external magnetic field.
- 2) Exciton tunneling direction is defined by the exciton

transitions energy difference in the adjacent QWs independently on the single-particle levels alignment. Thus, excitonic effects are absolutely important in charge transfer and determine the nature of tunneling in ADQWs with thermally induced disorder. In turn, it makes possible to control exciton tunneling direction with external magnetic field.

3) Absence of anticrossing behaviour of hh-excitons evidences about incoherent nature of hh-exciton tunneling and the absence of excitonic level interaction in ADQWs with strong short-range disorder, caused by the quick thermal annealing.

4) The simplest, rectangular shape model of ADQW band potential profile has proved to describe satisfactorily the magnetic field behavior of the hh- and lh-exciton states.

5) Interwell stress relaxes completely during rapid temperature annealing in the ADQWs with barriers $\gtrsim 4$ nm, leading to small values of hh-lh splitting Δ_{hh-lh} , while in structures with narrow barriers stress effects remain important.

6) Valence band-mixing effects in II-VI semiconductor ADQWs with strong excitonic effect and small Δ_{hh-lh}

are supposed as an underlaying physical factor for the effective exciton tunneling experimentally observed for different interwell alignment configurations. Elastic scattering via alloy composition fluctuations and interface defects are considered as the determinant tunneling mechanisms in the ternary ADQWs, subjected to the rapid temperature treatment.

In general, tunneling experiments in ADQWs, based on II-VI semimagnetic materials, have shown specificity of the tunneling phenomena in heterostructures made on these compounds. Strong excitonic correlations and valence band-mixing are supposed to govern the nature of interwell exciton transfer. Experimental data point that the role of valence band-mixing effects in exciton transfer should be reconsidered for II-VI semiconductor heterostructures with strong excitonic effect.

VI. ACKNOWLEDGMENTS

This work was supported by Russian Foundation for Basic Research, grant No. 04-02-17338.

* Electronic address: zaitsev@issp.ac.ru

¹ V.B. Timofeev, UFN **174**, 1109 (2004).

² L.V. Butov, A.C. Gossard, and D.S. Chemla, Nature **418**, 751 (2002).

³ L. V. Butov, A.L. Ivanov, A. Imamoglu, P.B. Littlewood, A.A. Shashkin, V. T. Dolgopolov, K.L. Campman, and A.C. Gossard, Phys. Rev. Lett. **86**, 5608 (2001).

⁴ L. Esaki, IEEE J Quantum Electron. **QE-22**, 1611 (1986).

⁵ S. Ten, F. Henneberger, M. Rabe, and N. Peyghambarian, Phys. Rev. B **53**, 12637 (1996).

⁶ R. Ferreira, P. Rolland, Ph. Roussignol, C. Delalande, A. Vinattieri, L. Carraresi, M. Colocci, N. Roy, B. Sermage, and J.F. Palmier, B. Etienne, Phys. Rev. B **45**, 11782 (1992).

⁷ D. Suisky, W. Heimbrot, C. Santos, F. Neugebauer, M. Happ, B. Lunn, J.E. Nicholls, and D.E. Ashenford, Phys. Rev. B **58**, 3969 (1998).

⁸ I. Galbraith and G. Duggan, Phys. Rev. B **40**, 5515 (1989).

⁹ W. Heimbrot, L. Gridneva, M. Happ, N. Hoffmann, M. Rabe, and F. Henneberger, Phys. Rev. B **58**, 1162 (1998).

¹⁰ W. Heimbrot, M. Happ, and F. Henneberger, Phys. Rev. B **60**, R16326 (1999).

¹¹ H. Falk, J. Hübner, P.J. Klar, and W. Heimbrot, Phys. Rev. B **68**, 165203 (2003).

¹² R. Ferreira, C. Delalande, H.W. Liu, and G. Bastard, B. Etienne, J.F. Palmier, Phys. Rev. B **42**, 9170 (1990).

¹³ D.Y. Oberly, J. Shah, T.C. Damen, C.W. Tu, T.Y. Chang, D.A.B. Miller, J.E. Henry, R.F. Kopf, N. Sauer, and Di-Giovanni, Phys. Rev. B **40**, 3028 (1989).

¹⁴ K. Leo, J. Shah, J.P. Gordon, T.C. Damen, D.A.B. Miller, C.W. Tu, J.E. Cunningham, Phys. Rev. B **42**, 7065 (1990).

¹⁵ M. Nido, M.G.W. Alexander, W.W. Rühle, and K. Köhler, Phys. Rev. B **43**, 1839 (1991).

¹⁶ A.P. Heberle, W.W. Rühle, and K. Köhler, Phys. Status Solidi B **173**, 381 (1992).

¹⁷ J. Seufert, M. Obert, G. Bacher, A. Forchel, T. Passow, K. Leonardi, and D. Hommel, Phys. Rev. B **64**, 121303 (2001).

¹⁸ M. K. Welsch, G. Bacher, H. Schmid, A. Forchel, S. Zaitsev, C. R. Becker, and L. W. Molenkamp, Phys. Status Solidi B **238**, 313 (2003).

¹⁹ R. Heitz, I. Mukhametzhanov, P. Chen, and A. Madhukar, Phys. Rev. B **58**, R10151 (1998).

²⁰ Yu.I. Mazur, Zh.M. Wang, G.G. Tarasov, G.J. Salamo, J.W. Tomm, V. Talalaev, and H. Kissel Phys. Rev. B **71**, 235313 (2005).

²¹ J. Shah, *Ultrafast Spectroscopy of Semiconductors and Semiconductor Nanostructures*, (Springer Series in Solid-State Sciences, vol. 115, 1999), ch. 7.

²² R. Ferreira and G. Bastard, Phys. Rev. B **40**, 1074 (1989).

²³ F. C. Michl, R. Winkler, and U. Rössler, Solid State Commun. **99**, 13 (1996).

²⁴ L. Kłopotowski, M. Nawrocki, S. Maćkowski, and E. Janik, Phys. Status Solidi B **229**, 769 (2003).

²⁵ F.T. Vasko and O.E. Raichev, Zh. Eksp. Teor. Fiz. **104**, 3103 (1993) [Sov.Phys. JETP **77**, 452 (1993)].

²⁶ I. Lawrence, S. Haacke, H. Mariette, W.W. Rühle, H. Ulmer-Tuffigo, J. Cibert, and G. Feuillet, Phys. Rev. Lett. **73**, 2131 (1994).

²⁷ A.P. Heberle, M. Oestreich, S. Haacke, W.W. Rühle, J. C. Maan, and K. Köhler, Phys. Rev. Lett. **72**, 1522 (1994).

²⁸ A.P. Heberle, W.W. Rühle, and K. Köhler, SPIE Proc: **1677**, 234 (1992).

²⁹ R. Ferreira, H.W. Liu, C. Delalande, J.F. Palmier and B. Etienne, Surf. Sci. **229**, 192 (1990).

³⁰ R. Wessel and M. Altarelli, Phys. Rev. B **39**, 12802 (1989).

³¹ E.T. Yu, M.K. Jackson, and T. C. McGill, Appl. Phys.

- Lett. **55**, 744 (1989).
- ³² E.E. Mendez, W.I. Wang, B. Ricco and L. Esaki, Appl. Phys. Lett. **47**, 415 (1985).
- ³³ M.K. Jackson, M.B. Johnson, D.H. Chow and T.C. McGill, Appl. Phys. Lett. **54**, 552 (1989).
- ³⁴ T. Takagahara, Phys. Rev. B **31**, 6552 (1985).
- ³⁵ A. Tomita, J. Shah, and R.S. Knox, Phys. Rev. B **53**, 10793 (1996).
- ³⁶ S.K. Lyo, Phys. Rev. B **62**, 13641 (2000).
- ³⁷ D.S. Kim, H.S. Ko, Y.M. Kim, S.J. Rhee, S.C. Hohng, Y.H. Yee, W.S. Kim, J.S. Woo, H.J. Choi, J. Ihm, D.H. Woo, and K.N. Kang, Phys. Rev. B **54**, 14580 (1996).
- ³⁸ D.S. Kim, H.S. Ko, Y.M. Kim, S.J. Rhee, S.C. Hohng, Y.H. Yee, W.S. Kim, J.S. Woo, H.J. Choi, J. Ihm, D.H. Woo, and K.N. Kang, Solid State Commun. **100**, 231 (1996).
- ³⁹ J.K. Furdyna, J. Appl. Phys. **64**, R29 (1988).
- ⁴⁰ D. Tönnies, G. Bacher, A. Forchel, A. Waag, and G. Landwehr, Appl. Phys. Lett. **64**, 5608 (2001).
- ⁴¹ T. Gurung, S. Maćkowski, H. E. Jackson, L. M. Smith, W. Heiss, J. Kossut, and G. Karczewski, Phys. Status Solidi B **241**, 652 (2003).
- ⁴² S. Zaitsev, M.K. Welsch, H. Schöming, G. Bacher, D.V. Kulakovskii, A. Forchel, B. König, C.R. Becker, W. Ossau, and L. W. Molenkamp, Semicond. Sci. Technol. **16**, 631 (2001).
- ⁴³ D.R. Yakovlev and K.V. Kavokin, Comments Condens. Matter Phys. **18**, 51 (1996).
- ⁴⁴ S.B Lev, V.I. Sugakov, and G.V. Vertsimakha, J. Phys.: Condens. Matter **16**, 4033 (2004).
- ⁴⁵ E.L. Ivchenko, P.E. Pikus, *Superlattices and Other Heterostructures. Symmetry and Optical Phenomena* (Springer, Berlin, 1997).
- ⁴⁶ C.Camilleri, F. Teppe, D. Scalbert, Y.G. Semenov, M. Nawrocki, M. Dyakonov, J. Cibert, S. Tatarenko, and T. Wojtowicz, Phys. Rev. B **64**, 085331 (2001).
- ⁴⁷ S.A. Crooker, D.D. Awschalom, J.J. Baumberg, F. Flack, and N. Samarth, Phys. Rev. B **56**, 7574 (1997).
- ⁴⁸ U. Jahn, M. Ramsteiner, R. Hey, H. T. Grahn, E. Runge, and R. Zimmermann, Phys. Rev. B **56**, R4387 (1997).
- ⁴⁹ B. Kuhn-Heinrich, W. Ossau, T. Litz, A. Waag, and G. Landwehr, J. Appl. Phys. **75**, 8046 (1994).
- ⁵⁰ M.K. Welsch, H. Schöming, M. Legge, G. Bacher, A. Forchel, B. König, C.R. Becker, W. Ossau, and L. W. Molenkamp, Appl. Phys. Lett. **78**, 2937 (2001).
- ⁵¹ J.A. Gaj, W. Grieshaber, C. Bodin-Deshayes, J. Cibert, G. Feuillet, Y. Merle d'Aubigné, and A. Wasiela, Phys. Rev. B **50**, 5512 (1994).
- ⁵² W. Grieshaber, A. Haury, J. Cibert, Y. Merle d'Aubigné, A. Wasiela, and J.A. Gaj, Phys. Rev. B **53**, 4891 (1996).
- ⁵³ A.A. Sirenko, T. Ruf, M. Cardona, D.R. Yakovlev, W. Ossau, A. Waag, and G. Landwehr, Phys. Rev. B **56**, 2114 (1997).
- ⁵⁴ R.P. Leavitt and J.W. Little, Phys. Rev. B **42**, 11774 (1990).
- ⁵⁵ G.E.W. Bauer and T. Ando, Phys. Rev. B **38**, 6015 (1988).
- ⁵⁶ W. Grieshaber, J. Cibert, J.A. Gaj, Y. Merle d'Aubigné and A. Wasiela, Phys. Rev. B **50**, 2011 (1994).
- ⁵⁷ D. Tönnies, G. Bacher, A. Forchel, A. Waag, Th. Litz, D. Hommel, Ch. Becker, G. Landwehr, M. Heuken, and M. Scholl, J. Cryst. Growth **138**, 362 (1994).
- ⁵⁸ S.C. Jain, M. Willander, and H. Maes, Semicond. Sci. Technol. **11**, 641 (1996).
- ⁵⁹ S. Maćkowski, Nguyen The Khoi, P. Kossacki, A. Golnik, J. A. Gaj, A. Lemaître, C. Testelin, C. Rigaux, G. Karczewski, T. Wojtowicz and J. Kossut, J. Cryst. Growth **184**, 966 (1998).
- ⁶⁰ T. Tada, A. Yamaguchi, T. Ninomiya, H. Uchiki, T. Kobayashi, and T. Yao, J. Appl. Phys. **63**, 5491 (1988).
- ⁶¹ S. Haacke, N.T. Pelekanos and H. Mariette, M. Zigone, A.P. Heberle, and W.W. Rühle, Phys. Rev. B **47**, 16643 (1993).
- ⁶² J. Tribollet, F. Bernardot, M. Menant, G. Karczewski, C. Testelin, and M. Chamarro, Phys. Rev. B **68**, 235316 (2003).
- ⁶³ W. Wang, A. Zunger, K.A. Mader, Phys. Rev. B **53**, 2010 (1996).
- ⁶⁴ P. Ray and P. K. Basu, Phys. Rev. B **45**, 9169 (1992).
- ⁶⁵ M.K. Welsch, H. Schöming, M. Legge, G. Bacher, A. Forchel, B. König, C.R. Becker, W. Ossau, and L.W. Molenkamp, Appl. Phys. Lett. **78**, 2937 (2001).
- ⁶⁶ D. Tönnies, G. Bacher, A. Forchel, A. Waag, and G. Landwehr, Appl. Phys. Lett. **64**, 766 (1994).
- ⁶⁷ A. Arnoult, J. Cibert, S. Tatarenko, and A. Wasiela, J. Appl. Phys. **87**, 3777 (2000).
- ⁶⁸ H. Cao, G. Klimovitch, G. Björk, and Y. Yamamoto, Phys. Rev. B **52**, 12184 (1995).
- ⁶⁹ J.W. Wu and A.V. Nurmikko, Phys. Rev. B **37**, 2711 (1988).
- ⁷⁰ S. Haacke, N.T. Pelekanos, H. Mariette, M. Zigone, A.P. Heberle, and W.W. Rühle, Phys. Rev. B **47**, 16643 (1993).
- ⁷¹ W.M. Chen, I.A. Buyanova, K. Kayanuma, K. Nishibayashi, K. Seo, A. Murayama, Y. Oka, A.A. Toropov, A.V. Lebedev, S.V. Sorokin, and S.V. Ivanov, Phys. Rev. B **72**, 073206 (2005).
- ⁷² M.A. Berding, Phys. Rev. B **60**, 8943 (1999).
- ⁷³ N. Krsmanovic, K.G. Lynn, M.H. Weber, R. Tjossem, Th. Gessmann, Cs. Szeles, E.E. Eissler, J.P. Flint, and H.L. Glass, Phys. Rev. B **62**, R16279 (2000).
- ⁷⁴ Yu.G. Kusrayev, A.V. Koudinov, B.P. Zakharchenya, W.E. Hagston, D.E. Ashenford, B. Lunn., Solid State Commun. **95**, 149 (1995).
- ⁷⁵ G.D. Sanders and Y.C. Chang, Phys. Rev. B **31**, 6892 (1985).
- ⁷⁶ R. Ferreira and G. Bastard, Europhys. Lett. **10**, 279 (1989).
- ⁷⁷ G. Bastard, J. A. Brum, and R. Ferreira, in *Solid State Physics: Advances in Research and Applications*, edited by H. Ehrenreich and D. Turnbull (Academic, New York, 1991), Vol. 44, ch. 12.
- ⁷⁸ T.B. Norris, N. Vodjani, B. Vinter, E. Costard, and E. Böckenhoff, Phys. Rev. B **43**, 1867 (1991).
- ⁷⁹ B.P. Zakharchenya, P.C. Kop'ev, D.N. Mirlin, D.G. Polacov, I.I. Reshina, V.F. Sapega, and A.A.Sirenko, Solid State Commun. **69**, 203 (1989).
- ⁸⁰ T.C. Damen, J. Shah, D.Y. Oberli, D.S. Chemla, J.E. Cunningham, and J.M. Kuo, Phys. Rev. B **42**, 7434 (1990).